Patterns of Nonadditivity between Pairs of Stability Mutations in Staphylococcal Nuclease†

Susan M. Green‡ and David Shortle*

Department of Biological Chemistry, The Johns Hopkins University School of Medicine, Baltimore, Maryland 21205

Received May 5, 1993; Revised Manuscript Received June 28, 1993•

ABSTRACT: To identify interactions between amino acid positions in staphylococcal nuclease that affect its stability, a collection of 71 double-mutant forms was constructed from 22 previously characterized single mutants. These single mutations were assigned to three different classes on the basis of their m value [$m = d(\Delta G)/d[GuHCl]$], a parameter that has been correlated with energetically significant changes in the structure of the denatured state [Green et al. (1992) *Biochemistry 31*,5717–5728]. Several mutant pairs from five of the six possible double-mutant classes were analyzed by guanidine hydrochloride denaturation to determine the extent to which changes in stability ($\Delta\Delta G_{H_2O}$) and changes in the m value (Δm_{GuHCl}) reflect the sum of the effects of the individual mutants. The differences between the values for $\Delta\Delta G_{H_2O}$ and Δm_{GuHCl} estimated on the assumption of additivity and those obtained by experiment, i.e., $\Delta\Delta\Delta G$ and $\Delta\Delta m$, were calculated for each double-mutant protein. Surprisingly, a large majority of double mutants from four of the five classes exhibited positive values of $\Delta\Delta\Delta G$ and $\Delta\Delta m$; i.e., they were more stable and displayed a higher sensitivity to GuHCl than predicted on the basis of additivity. Statistical analysis of the data reveals (1) a highly significant correlation between the value of $\Delta\Delta\Delta G$ (the nonadditivity in stability) and $\Delta\Delta m$ (the nonadditivity in GuHCl sensitivity), (2) only weak correlations between the distance separating two mutant positions and the magnitude of $\Delta\Delta\Delta G$ and $\Delta\Delta m$, (3) evidence for unique patterns of interactions between some pairs of mutations, and (4) a triad of positions remote in sequence but relatively close in the native structure that show a dramatic degree of nonadditivity. The proposal is made that, for some mutants, the dominant pathway of interaction between widely separated positions involves changes in the residual structure of the denatured state, structure which retains a cooperative character and can extend out 20 or more angstroms.

Over the past 10 years, extensive use has been made of single mutations as probes of the roles of individual amino acid residues in specifying the folded structures and stabilities of proteins (Matthews, 1987; Goldenberg, 1988; Shortle, 1989, 1992). Quantitation of the change in stability $\Delta\Delta G_{H_2O}$ accompanying the substitution of a residue provides some measure of the contribution of the wild-type side chain to the overall balance of interactions that maintain the stability of the folded state. Single mutations, however, cannot probe for interactions between pairs of residues. To address this issue, double mutants can be constructed and the measured energetic consequences compared to the sum of the effects of the two single mutations (Ackers & Smith, 1985; Shortle & Meeker, 1986; Wells, 1990; Serrano et al., 1991; Mildvan et al., 1992). When there is close agreement between the observed $\Delta\Delta G_{H_2O}$ and that predicted on the assumption of additivity, by definition the two mutations exert their effects independently. In other words, the effect of a mutation at position A does not depend on energy terms that can be modified by a change in the amino acid at position B and vice versa. When the predicted and observed effects do not agree, the effect of one of the mutations must depend on an energy term that has been modified by the other mutation. In this case, the two mutations are considered interdependent, and the modified energy term can be presumed to reflect some sort of conformational or structural change that mediates interaction or "communication" between the two positions.

Only a limited number of studies of paired mutant effects on protein stability have been reported, with the general conclusion being that effects often appear to be additive within the limits of experimental error (Sandberg & Terwilliger, 1989; Shirley et al., 1989; Wells, 1990). However, an earlier study by this laboratory of double mutations in staphylococcal nuclease revealed that two of four double mutants were significantly more unstable than predicted from adding the effects of the single mutations (Shortle & Meeker, 1986). In addition to being less stable than wild type, all of the single mutations in that study displayed significant changes in m_{GuHCl}, a parameter that is defined as the rate of change of ΔG with respect to GuHCl concentration and reflects the sensitivity of the denaturation reaction to changes in denaturant concentration. Interestingly, the two nonadditive double mutants involved pairs of m$^-$ mutants (mutant $m_{GuHCl} < 0.95$ wt m_{GuHCl}), whereas the two additive double mutants involved pairs of m$^+$ mutants (mutant $m_{GuHCl} > 1.05$ wt m_{GuHCl}).

Studies of these and similar mutations have led us and others to the conclusion that the changes in m_{GuHCl} reflect changes in the residual structure of the denatured state (Shortle & Meeker, 1986, 1989; Shortle et al., 1990; Green et al., 1992; Shortle, 1993; Bowler et al., 1993). Ten different m$^+$ mutants in large denatured fragments of staphylococcal nuclease have consistently shown a reduction in residual structure relative to the wild-type fragment on the basis of far ultraviolet circular dichroism spectra and hydrodynamic radius, whereas similar studies on m$^-$ mutants have identified several that increase this residual structure, although a majority show only small

† This work was supported by NIH Grant GM34171 (D.S.) and by NIH Postdoctoral Fellowship GM14306 (S.M.G.).

* Author to whom correspondence should be addressed.

‡ Present address: Department of Biophysics and Biophysical Chemistry, The Johns Hopkins University School of Medicine, Baltimore, MD 21205.

• Abstract published in *Advance ACS Abstracts,* September 1, 1993.

0006-2960/93/0432-10131$04.00/0

changes (Shortle & Meeker, 1989; unpublished data). In view of this direct evidence for structural changes in this fragment model of the denatured-state, we proposed that the mechanism responsible for the observed nonadditivity between mutant pairs could involve changes in denatured state structure (Shortle & Meeker, 1986).

To extend the data available on mutant–mutant interactions in staphylococcal nuclease and to more thoroughly address the possibility that large conformational changes in the denatured state provide a common mechanism for nonadditive stability effects in this small protein, we have now examined 71 mutant pairs in which different pairs of m^+, m^-, and m^0 (0.95 wt m_{GuHCl} < mutant m_{GuHCl} < 1.05 wt m_{GuHCl}) mutants have been combined. Here we report the finding of frequent nonadditive interactions between stability mutants at a number of positions, some quite remote in the native folded structure. On the basis of several dominant trends in these data, we propose a simple model for the types of changes in denatured-state structure that may underlie these interactions.

MATERIALS AND METHODS

Recombinant DNA. All mutants of staphylococcal nuclease were generated using the Kunkel (1985) method of oligonucleotide-directed mutagenesis applied to the M13 phage vector MFO9, which carries the wild-type nuclease gene. After transformation of mutagenized DNA into competent DH5αF′ cells, plaques were picked, the phage DNA was sequenced, and the mutant nuclease gene moved into the expression plasmid pλ12 (Shortle et al., 1990). To ensure that no spurious secondary mutations had been introduced, the entire nuclease gene was sequenced for each mutant. In addition, when results from denaturation experiments raised questions about the identity of a double or triple mutant, the nucleotide sequence was confirmed by sequencing the gene in the plasmid DNA.

Protein Isolation. Mutant proteins were purified from *Escherichia coli* strain AR120 carrying the appropriate mutant plasmid (Shortle et al., 1990). The concentration of purified nuclease was determined using the extinction coefficient of 0.93 cm^{-1} mg^{-1} mL at 280 nm for a 1 mg/mL solution (Fuchs et al., 1967). Protein purity was analyzed by SDS–PAGE, followed by staining with Coomassie Brilliant Blue R-250. All protein preparations were estimated to be at least 95% pure.

Guanidine Hydrochloride Denaturation. To quantitate the changes in stability due to one or more mutations, the intrinsic fluorescence of the single tryptophan at position 140 was measured as a function of guanidine hydrochloride concentration at 20°C and pH 7.0 as in Green et al. (1992).

RESULTS

Denaturation Data and Estimation of Errors. The positions of the 22 single mutations used in different pairwise combinations are shown in Figure 1 relative to the folded structure of staphylococcal nuclease. On the basis of its m_{GuHCl} (normalized to the wild-type value of –6.8 kcal mol^{-1} (M GuHCl)$^{-1}$, which is defined as 1.00), each of these mutations was assigned to one of the three *m*-value classes: $m^- < 0.95 < m^0 < 1.05 < m^+$. The values of $\Delta\Delta G_{H_2O}$ (the change in stability = $\Delta G_{H_2O,mutant} - \Delta G_{H_2O,WT}$) and Δm_{GuHCl} (the relative change in $d(\Delta G_{H_2O})/d[GuHCl] = m_{GuHCl,mutant} - m_{GuHCl,WT}$) for each single mutant are listed in Table I. In Table II, the 71 double mutants are grouped according to the *m*-value classes of the two single mutations. Both the $\Delta\Delta G_{H_2O}$ and Δm_{GuHCl} for each double mutant as well as the nonadditivity of the stability change $\Delta\Delta\Delta G$ [= $\Delta\Delta G_{H_2O,1+2} - (\Delta\Delta G_{H_2O,1} + \Delta\Delta G_{H_2O,2})$] and the nonadditivity of the *m*-value change $\Delta\Delta m$ [= $\Delta m_{GuHCl,1+2} - (\Delta m_{GuHCl,1} + \Delta m_{GuHCl,2})$] are also given in Table II. In addition, C_α–C_α and C_β–C_β distances for each pair of mutations are listed.

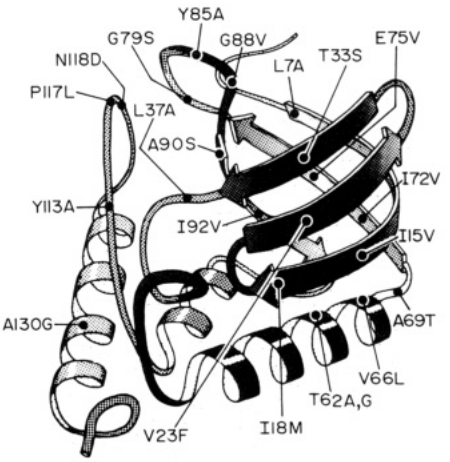

FIGURE 1: Ribbon diagram of the three-dimensional structure of staphylococcal nuclease with marked positions for all single mutations used in this study. Reproduced with permission from Richardson (1981). Copyright 1981 Academic Press.

Table I: Denaturation Data for Single Mutants

mutant	$\Delta\Delta G_{H_2O}$[a]	m_{GuHCl}[b]
class m^0		
115V[d]	–0.81	1.05
172V[d]	–1.77	1.02
Y85A[d]	–0.41	1.01
192V[d]	–0.50	1.01
Y113A[d]	0.03	0.99
A130G[e]	–1.11	0.96
class m^-		
L7A[d]	–1.58	0.89
V23F	–2.30	0.84
L37A[d]	–1.68	0.89
T62A[e]	–2.40	0.88
V66L[f]	–0.10	0.82
E75V	–2.31	0.79
G79D	–2.28	0.87
G79S[c]	–2.66	0.82
G88V[f]	–0.90	0.78
P117L	0.20	0.92
N118D	–2.40	0.86
class m^+		
118M[f]	–0.50	1.07
T33S	–1.00	1.09
T62G[e]	–3.48	1.08
A69T[f]	–2.63	1.13
A90S[f]	–1.90	1.10

[a] $\Delta\Delta G_{H_2O} = \Delta G_{H_2O,mutant} - \Delta G_{H_2O,WT}$. Units are kilocalories per mole. [b] Units are relative to the wild-type value of 6.85 kcal mol^{-1} M^{-1}, which has been normalized to 1.00. [c] Shortle (1986). [d] Shortle et al. (1990). [e] Green et al. (1992). [f] Shortle and Meeker (1986).

To estimate the range of error in the values of $\Delta\Delta G_{H_2O}$ and Δm_{GuHCl}, 25 double mutants were selected at random and the denaturation was repeated. Comparison of the two values indicated that $\Delta\Delta G_{H_2O}$ varied by 0.09 ± 0.08 kcal/mol and Δm_{GuHCl} varied by 0.02 ± 0.01 unit, where the units are normalized relative to the wild-type value. [These ranges of error are slightly higher than have been found in other such analyses (Green et al., 1992).] Since three different experimental values of $\Delta\Delta G_{H_2O}$ and Δm_{GuHCl} are required to calculate the two nonadditivity parameters $\Delta\Delta\Delta G$ and $\Delta\Delta m$, the error levels in these parameters are estimated as approximately ±0.3 kcal/mol and ±0.05 relative *m* unit, respectively.

Table II: Denaturation Data for Double Mutants

mutant	$\Delta\Delta G_{H_2O}$[a]	m_{GuHCl}[b]	$\Delta\Delta\Delta G$[c]	$\Delta\Delta m$[d]	C_α–C_α[e]	C_β–C_β[e]
$m^0 \times m^0$						
15V+72V	–2.01	1.12	0.57	0.05	11.2	10.54
15V+85V	–1.06	1.09	0.16	0.03	18.56	17.15
15V+113A	–0.62	1.08	0.16	0.04	27.95	28.23
72V+85A	–1.6	1.07	0.58	0.04	22.78	21.36
72V+113A	–0.94	1.1	0.8	0.09	25.66	26.3
85A+113A	–0.23	1.04	0.15	0.04	17.71	16.66
$m^+ \times m^+$						
18M+33S	–2	1.09	–0.5	–0.07	8.85	7.09
18M+69T[f]	–3.3	1.26	–0.2	0.06	16.39	16.29
18M+90S[f]	–2.7	1.16	–0.3	–0.01	15.47	14.52
33S+90S	–3.16	1.2	–0.26	0.01	10.59	10.98
69T+90S	–4.7	1.3	–0.17	0.07	17.45	15.09
$m^- \times m^-$						
7A+23F	–3.65	0.71	0.23	–0.02	20.51	18.74
7A+37A	–1.65	0.88	1.61	0.1	13.81	10.97
7A+75V	–3.64	0.73	0.25	0.05	6.66	5.44
7A+79S	–2.77	0.8	1.47	0.09	11.06	NA
23F+37A	–3.17	0.73	0.81	0.0	11.8	12.14
23F+75V	–4.79	0.58	–0.18	–0.05	13.94	13.5
23F+79S	–4.75	0.59	0.21	–0.07	20.19	NA
37A+75V	–2.47	0.79	1.52	0.11	9.83	8.5
37A+79S	–1.83	0.87	2.51	0.16	11.3	NA
37A+117L	–1.69	0.85	–0.21	0.04	11.89	11.73
37A+118D	–1.72	0.91	2.36	0.16	8.06	6.2
62A+66L	–2.4	0.68	0.1	–0.02	6.37	6.52
62A+88V	–3.2	0.69	0.1	0.03	16.64	NA
66L+88V[f]	–2.0	0.57	–1.0	–0.03	16.52	NA
75V+79S	–4.67	0.56	0.3	–0.05	11.87	NA
75V+117L	–1.61	0.78	0.5	0.07	14.33	14.25
79S+117L	–2.08	0.87	0.38	0.13	5.28	NA
79D+118D	–2.58	0.85	2.10	0.12	5.21	NA
79S+118D	–2.79	0.84	2.27	0.16	5.21	NA
117L+118D	–1.0	0.86	1.20	0.08	3.87	5.87
37/79/118	–1.64	0.91	5.10	0.34	NA	NA
37/79/117	–1.83	0.85	2.31	0.22	NA	NA
79/117/118	–2.94	0.74	1.92	0.14	NA	NA
$m^- \times m^+$						
23F+33S	–2.72	1.03	0.58	0.1	5.86	7.7
23F+69T	–4	1.17	0.93	0.20	13.65	11.02
23F+90S	–3.31	1.06	0.89	0.12	10.79	9.69
37A+33S	–2.21	1.01	0.47	0.03	12.54	13.53
37A+69T	–4.13	1.09	0.18	0.07	19.54	18.14
37A+90S	–3.32	1.02	0.26	0.03	5.19	5.86
75V+33S	–3.21	0.89	0.10	–0.01	14.05	16.36
75V+69T	–4.35	1.03	0.59	0.11	14.64	16.29
75V+90S	–3.6	0.97	0.61	0.08	5.4	5.67
62G+88V	–3.66	0.96	0.72	0.1	16.64	NA
$m^- \times m^0$						
7A+15V	–2.08	0.96	0.31	0.02	23.85	23.36
7A+72V	–2.41	1.01	0.94	0.1	15.87	16.15
7A+85A	–1.6	0.95	0.39	0.05	23.29	22.83
7A+92V	–1.54	0.96	0.54	0.06	12.51	12.91
7A+113A	–1.1	0.96	0.45	0.08	20.99	20.8
7A+130G	–2.46	0.87	0.23	0.02	25.05	23.44
23F+15V	–2.59	0.96	0.52	0.07	7.81	8.23
23F+72V	–2.9	0.95	1.17	0.09	11.35	8.65
23F+85A	–2.51	0.86	0.2	0.01	13.89	14.29
23F+92V	–2.01	0.96	0.79	0.11	9.37	6.6
23F+113A	–1.89	0.91	0.38	0.08	20.32	20.97
23F+130G	–3.5	0.76	–0.09	–0.04	25.57	25.8
37A+15V	–2.17	1.01	0.32	0.07	18.78	19.1
37A+72V	–2.78	1.01	0.67	0.1	15.59	15.12
37A+85A	–1.98	0.9	0.11	0	14.08	14.31
37A+92V	–1.77	0.99	0.41	0.09	8.62	8.59
37A+113A	–1.46	0.92	0.19	0.04	10.31	11.92
37A+130G	–2.53	0.89	0.26	0.04	18.07	18.89
75V+15V	–2.83	0.87	0.29	0.03	17.39	18.35
75V+72V	–3.12	0.9	0.96	0.09	10.29	10.99
75V+85A	–2.51	0.82	0.21	0.02	18.95	19.93
75V+92V	–2.05	0.91	0.76	0.11	6.4	7.6
75V+113A	–1.55	0.92	0.73	0.14	19.3	20.07
75V+130G	–3.4	0.74	0.02	–0.01	23.78	22.75
79S+15V	–3.1	0.95	0.37	0.08	25.26	NA
79S+72V	–3.61	0.98	0.82	0.14	21.66	NA
79S+85A	–2.69	0.89	0.38	0.06	16.06	NA
79S+92V	–2.55	0.93	0.61	0.1	16.13	NA
79S+113A	–2.22	0.93	0.41	0.12	14.91	NA
79S+130G	–3.68	0.76	0.09	–0.02	25.75	NA

[a] $\Delta\Delta G_{H_2O} = \Delta G_{H_2O,mutant} - \Delta G_{H_2O,WT}$. Units are kilocalories per mole. [b] Units are relative to the wild-type value of 6.85 kcal mol^{-1} M^{-1}, which has been normalized to 1.00. [c] $\Delta\Delta\Delta G = \Delta\Delta G_{H_2O,mutant\ 1+2} - (\Delta\Delta G_{H_2O,mutant\ 1} + \Delta\Delta G_{H_2O,mutant\ 2}$. [d] $\Delta\Delta m = \Delta m_{GuHCl,mutant\ 1+2} - (\Delta m_{GuHCl,mutant\ 1} + \Delta m_{GuHCl,mutant\ 2})$. [e] Distances measured from coordinates of Hynes and Fox (1991). [f] Shortle and Meeker (1986).

Six double mutants (V23F+E75V, V23F+G79S, L37A+A69T, A69T+A90S, E75V+A69T, E75V+G79S) were significantly denatured even in the absence of denaturant. In these cases, ΔG_{H_2O} was determined by ammonium sulfate renaturation, and this value was used as one of the data points in the linear least-squares fitting to obtain m_{GuHCl} (Shortle et al., 1990).

The $m^0 \times m^0$ Class. Four single mutants, I15V, I72V, Y85A, and Y113A, from the m^0 class were recombined pairwise to give the six possible double-mutant combinations. As can be seen for the values listed in Table II, in all cases the value of $\Delta\Delta\Delta G$ is positive, ranging from 0.15 to 0.80 kcal/mol. Thus, all of these double mutants are more stable than predicted from the assumption of additive effects, although for only three of the six is $\Delta\Delta\Delta G$ outside the range of estimated error (±0.3 kcal/mol). Likewise, the value of $\Delta\Delta m$ is positive in all six cases, ranging from 0.03 to 0.09 (±0.05 is the estimated error). From this sample it appears that the property of being an m^0 mutant is not conserved; each of the double mutants is classified as an m^+ mutant by the criteria listed above.

It is noteworthy that the double mutant in this class which displays the largest nonadditivity in both stability and m value, I72V+Y113A, involves two widely separated residues. In the wild-type native state, the alpha carbons are 25.7 Å apart, and the beta carbons are 26.3 Å apart, which literally places these two residues on opposite sides of the molecule. To address the more general issue of whether nonadditive effects tend to be more pronounced for residues close together in the wild-type native structure, correlations were sought between the two nonadditivity parameters and the distance between mutant positions. Although the sample size is small, the C_β–C_β distance did not correlate with either $\Delta\Delta\Delta G$ ($r = 0.0750$, $p = 0.888$) or $\Delta\Delta m$ ($r = 0.3499$, $p = 0.497$).

However, as shown in Figure 2A, a weak correlation was found between $\Delta\Delta\Delta G$ and $\Delta\Delta m$ ($r = 0.7930$, $p = 0.060$, slope = 10.5 kcal mol^{-1} m-$unit^{-1}$). Although the statistical significance of this correlation is marginal at best, a similar correlation was found for each of the other four classes of double mutants and will be discussed at length below.

The $m^+ \times m^+$ Class. Four m^+ mutants, I18M, T33S, A69T, and A90S, were recombined to give five of the six possible pairs (T33S+A69T is missing). For this class of double mutants, $\Delta\Delta\Delta G$ was never observed to be positive; instead, the range fell from –0.17 to –0.5 kcal/mol. $\Delta\Delta m$ ranged from –0.07 to 0.07 with three of the double mutants considered nonadditive. The correlation between the C_β–C_β distance for each residue and $\Delta\Delta\Delta G$ and $\Delta\Delta m$ is slightly significant with $r = 0.8803$, $p = 0.049$ and $r = 0.8624$, $p = 0.06$, respectively.

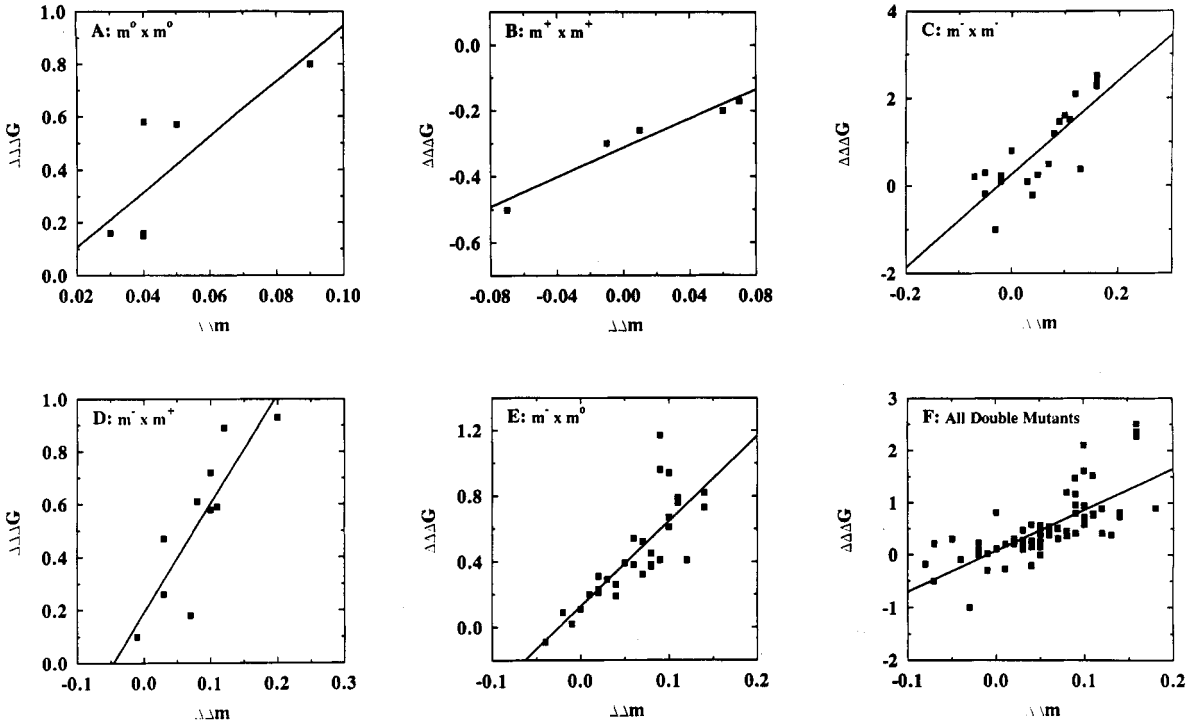

FIGURE 2: Scatterplots of the nonadditivity in stability ($\Delta\Delta\Delta G$) vs the nonadditivity in m_{GuHCl} ($\Delta\Delta m$) for six groups of double mutants. The solid line represents the best linear least-squares fit to the data; the correlation coefficients and statistical significance are given in the text. $\Delta\Delta\Delta G$ is expressed in kilocalories per mole and $\Delta\Delta m$ in units normalized relative to the value of m_{GuHCl} for wild-type nuclease, –6.8 kcal mol^{-1} (M of GuHCl)$^{-1}$.

A clearly significant correlation was found, however, between $\Delta\Delta\Delta G$ and $\Delta\Delta m$ ($r = 0.9719, p = 0.006$, slope = 2.22 kcal mol^{-1} m-unit^{-1}) (Figure 2B). As discussed below, this correlation probably reflects a statistical artifact referred to as the "isokinetic effect".

The m⁻ × m⁻ Class. A total of 20 double mutants were analyzed in this class. Five m⁻ mutants, L7A, V23F, L37A, E75V, and G79S, were recombined pairwise to give the 10 possible double mutants; in addition, N118D was paired with three from the above group and P117L with two from the above group and with N118D. Finally, the three m⁻ mutants, T62A, V66L, and G88V, were recombined with each other to give three additional double mutants.

In this class of double mutants, nonadditive effects are common (11 of 20) and often dramatic. $\Delta\Delta\Delta G$ ranged from –1.0 to 2.5 kcal/mol and $\Delta\Delta m$ from –0.07 to 0.16. However, the clear trend is for $\Delta\Delta\Delta G$ to be positive, since only one mutant (V66L+G88V) has a negative value that is significantly greater than the level of error. For this larger data set there may be a weak correlation between the magnitude of the nonadditivity parameters and the distance separating the two mutant sites. Since two wild-type glycines have been mutated in this mutant set, distances between C_α atoms were analyzed and found to correlate with $\Delta\Delta\Delta G$ ($r = -0.4659, p = 0.038$) and with $\Delta\Delta m$ ($r = -0.6008, p = 0.005$). However, in the 11 cases for which the C_β–C_β distance is defined, no significant correlation is found with either $\Delta\Delta\Delta G$ ($r = -0.3997$, $p = 0.223$) or $\Delta\Delta m$ ($r = -0.4842$, $p = 0.131$).

As found for the previous two groups and shown in Figure 2C, a significant correlation exists between $\Delta\Delta\Delta G$ and $\Delta\Delta m$ ($r = 0.8157, p < 0.0005$). In this case the slope of the regression curve that expresses the dependence of $\Delta\Delta\Delta G$ on $\Delta\Delta m$ is 10.6 kcal mol^{-1} m-unit^{-1}, similar to that for the m⁰ × m⁰ class but much larger than that for the m⁺ × m⁺ class.

For mutations involving the three residue positions L37, G79, and N118, the nonadditivity is dramatic: (1) When mutation G79S is added to mutation L37A, it effectively disappears, $\Delta\Delta G_{H_2O}$ and Δm_{GuHCl} of the double mutant being indistinguishable from those of L37A. (2) Similarly, when N118D is added to mutation L37A, it also has no additional effects. (3) When N118D is added to G79S, it disappears as well. A second mutation at position 79, G79D, also displays striking nonadditivity with N118D, although in this case there may be a small effect of the N118D mutation on the double mutant. However, L37A and G79S do not show identical nonadditive behavior with all other mutations. Whereas L37A masks more than half of the effect of mutation E75V, G79S exhibits nearly additive behavior when paired with E75V.

Three triple mutants were constructed to further probe the interactions between these three positions plus position 117. Triple mutant L37A+G79S+N118D maintains the trends seen for the three double mutants; within the limits of error, it is essentially indistinguishable from L37A. The stability effects of both G79S and N118D have disappeared! Since both G79 and N118 are positioned within a few angstroms of the *cis*-proline at position 117 in the wild-type native structure, we sought to remove this structural feature by adding mutation P117L to the two double mutants L37A+G79S and G79S+N118D. Replacement of this proline with leucine has only a very small effect on stability, even though it can be assumed to force the peptide bond between 116 and 117 into the trans configuration. Within the limit of measurement error, it appears that the P117L mutation has no effect on the nonadditivity phenomena involving these three positions. However, the P117L mutation has a range of effects in combination with the three single mutants: the destabilizing effect of N118D is reduced by 50%, the effect of G79S may be slightly reduced, but the destabilizing effect of L37A is unchanged.

The m⁻ × m⁺ Class. The 10 double mutants in this class consist of each of the three m⁻ mutants, V23F, L37A, and E75V, recombined with each of the three m⁺ mutants, T33S,

A69T, and A90S, plus the pair T62G+G88V. For all members of this class, $\Delta\Delta\Delta G$ is either zero or positive (up to 0.9 kcal/mol), with seven of the mutant pairs showing a significant level of nonadditivity. In addition, $\Delta\Delta m$ is positive in all cases except one (E75V+T33S, $\Delta\Delta m = -0.01$), which is not significantly different from zero.

Again, no correlation is demonstrated between the distance separating the two residues in the wild-type structure as measured by the C_β–C_β distance and the value of either $\Delta\Delta\Delta G$ ($r = -0.3815$, $p = 0.311$) or $\Delta\Delta m$ ($r = -0.1657$, $p = 0.670$). The double mutant L37A+A90S displays essentially additive behavior, even though its beta carbons are only 5.86 Å apart in the wild-type native state, whereas for the most significantly nonadditive pair, V23F+A69T, the beta carbons are separated by 11.0 Å.

For this class of double mutants, a correlation is again found between $\Delta\Delta\Delta G$ and $\Delta\Delta m$ as shown in Figure 2D. In this case, $r = 0.8556$, $p = 0.002$, and the slope of $\Delta\Delta\Delta G$ expressed as a function of $\Delta\Delta m$ is 4.1 kcal mol^{-1} m-unit^{-1}.

The m^- × m^0 Class. A total of 30 pairs of mutants were constructed by recombining each of five m^- mutants, L7A, V23F, L37A, E75V, and G79S, with each of six m^0 mutants, I15V, I72V, Y85A, I92V, Y113A, and A130G. For all double mutants except 1 (V23F+A130G), $\Delta\Delta\Delta G$ was positive, varying from –0.09 to 1.17 kcal/mol, with 19 being greater than 0.3 kcal/mol. For all doubles except three, $\Delta\Delta m$ was also positive, with the total range of values extending from –0.04 to 0.14.

Nonadditivity does not appear to be a random property of the m^0 mutants. For the two mutants I72V and I92V, each combination with the five m^- mutants displays significant nonadditivity, whereas none of the pairs involvin A130G and only two involving Y85A show comparable nonadditivity. The fact that all five m^- mutants are nonadditive in either three or four of the six pairs suggests that the identity of the m^0 mutant plays a greater role in the occurrence of nonadditivity than does the m^- mutant.

For the 30 members of this class, a weak but significant correlation can be demonstrated between the two nonadditivity parameters and the distance separating the mutant sites. $\Delta\Delta\Delta G$ correlates with both the C_β–C_β distance ($r = -0.5869$, $p = 0.003$) and the C_α–C_α distance ($r = -0.4905$, $p = 0.006$), as does $\Delta\Delta m$ ($r = -0.5253$, $p = 0.008$, and $r = -0.4228$, $p = 0.020$, respectively).

For this large double-mutant class, the correlation between $\Delta\Delta\Delta G$ and $\Delta\Delta m$ is both relatively strong and highly significant, $r = 0.8139$, $p < 0.0005$. The functional dependence of $\Delta\Delta\Delta G$ on $\Delta\Delta m$ in this case is 5.2 kcal mol^{-1} m-unit^{-1}.

The Class of All Double Mutants. When all 71 double mutants are analyzed as a single set, a weak correlation is seen between the two measures of residue separation in the wild-type folded state and both nonadditivity parameters. $\Delta\Delta\Delta G$ can be correlated with both C_β–C_β ($r = -0.3087$, $p = 0.022$) and C_α–C_α ($r = -0.3515$, $p = 0.003$), whereas the two correlations with $\Delta\Delta m$ are very marginal at best ($r = -0.2324$, $p = 0.088$, and $r = -0.2701$, $p = 0.023$, respectively). Although all five classes exhibited a correlation between $\Delta\Delta\Delta G$ and $\Delta\Delta m$, the value of the slope for this relationship varied by almost a factor of 3. As discussed below, this observation suggests that there must be different mechanisms underlying this correlation for different double-mutant classes. Therefore, it may be inappropriate to group all data bearing on this correlation into a common category. Nevertheless, in the interest of completeness, when all of the double mutants are combined, the correlation between $\Delta\Delta\Delta G$ and $\Delta\Delta m$ is found to have $r = 0.7138$, $p < 0.0005$, with a slope of 7.7 kcal mol^{-1} m-unit^{-1}.

DISCUSSION

The most significant results presented above are the striking prevalence of nonadditive effects on stability and the finding that these effects are almost exclusively subadditive—two destabilizing mutations in the same protein lower its stability by an amount that is significantly less than the sum of the effects of the two single mutations. Although most previous studies of multiple mutants in T4 lysozyme (Zhang et al., 1991, 1992; Dao-pin et al., 1991; Eriksson et al., 1992), ribonuclease T1 (Shirley et al., 1989), dihydrofolate reductase (Perry et al., 1989), and other simple single-domain proteins (Stearman et al., 1988) have not uncovered such extensive nonadditivity, in some of these cases, the relatively large uncertainties in the measured values of $\Delta\Delta G_{H_2O}$ may have concealed changes of $\Delta\Delta\Delta G$ of less than 1 kcal/mol. Several clear instances of nonadditive effects have been found in barnase for neighboring residues involved in ionic pairing interactions (Serrano et al., 1990; Horovitz et al., 1990).

As discussed by Ackers and Smith (1985), when two mutations are independent, their effects are additive; neither mutation alters any parameter that plays a role in determining the effect of the other. When two mutations are nonadditive, some mechanism for communication between the two positions must exist. To phrase this in more molecular terms, each mutation causes a "sphere of perturbation", centered on the mutant side chain and extending out a variable distance into the surrounding structure (Ackers & Smith, 1985). When these spheres overlap in the double-mutant structure, by definition the structural/energetic effects of one mutation may be altered through perturbation of interactions in this region.

In this conceptual framework, the prevalence of the small, subadditive effects described above imply that mutations in staphylococcal nuclease often have large spheres of perturbation, since for a majority of mutant pairs, there is evidence of nonadditivity. The energetic consequences of such overlap tend to be small, resulting in an average deviation from additivity of approximately 0.5–1 kcal/mol. However, for mutants at sites 37, 79, and 118 the energetic consequences of this overlap involve several kilocalories per mole. To make any chemical sense of these observations, the central question that must be answered is, "What is the structure (or structures) in this protein that is so easily perturbed, leading to nonadditive effects on stability?"

The most obvious candidate is the folded native conformation. Considering how well-packed and extensively hydrogen-bonded the native state of most proteins is, with staphylococcal nuclease being no exception (Loll & Lattman, 1989; Hynes & Fox, 1991), it seems reasonable that a mutation at one site could give rise to changes that propagate a considerable distance out into the surrounding structure. But recent results of X-ray crystallography of mutant proteins, especially the T4 lysozyme system, do not support the notion that the native state is an extensively deformable structure. For a large majority of substitution mutations, the observed structural differences from wild type tend to be both small and confined to the immediate vicinity of the altered side chain [reviewed in Shortle (1992)]. Nevertheless, small perturbations of structure that may be energetically significant are occasionally seen at sites relatively remote from the mutation.

Since the reaction under study involves the equilibrium interconversion of two states, the native state (N) and the denatured state (D), the only alternative structure that could mediate these nonadditive effects is the denatured state. In recent years, structural characterization of denatured proteins has clearly indicated that considerable residual structure can persist and that the amount and type of structure depend sensitively on conditions of solution (Dill & Shortle, 1991). It is relevant here that staphylococcal nuclease denatures at relatively low concentrations of denaturant (<1 M GuHCl). Consequently, the denatured state formed under such mild conditions is expected to retain many significant chain–chain interactions, leading to large deviations from random coil behavior.

Over the past several years, this laboratory has presented several lines of evidence that suggest the residual structure of the denatured state of staphylococcal nuclease also depends sensitively on the amino acid sequence (Shortle & Meeker, 1989). Central to these arguments has been the observation that single amino acid substitutions, even relatively conservative ones, can lead to large deviations of m_{GuHCl} away from the value for wild type (Shortle & Meeker, 1986). All evidence to date indicates that the denatured state of m^+ mutants has a less structured D state, with a greater exposure of nonpolar residues to solvent. The structural changes responsible for m^- mutants are much less clear, although for a few such mutants it appears the D state is more structured, with a diminished exposure of nonpolar residues to solvent (Shortle & Meeker, 1989). Nevertheless, the simplest working assumption is that changes in m_{solute} [where solute can be GuHCl, urea, SCN^-, or polyols (Shortle et al. (1989)] are manifestations of changes in the solvation of the D state. The demonstration of a significant correlation between changes in m_{GuHCl} and changes in stability supports the conclusion that these changes in D-state structure are energetically important (Shortle et al., 1990), accounting for approximately half of the stability loss accompanying an average mutation in staphylococcal nuclease (Green et al., 1992).

If the structure that mediates the spheres of perturbation invoked to explain this prevalent nonadditivity is in fact the residual structure of the D state, then one would expect to find a correlation between nonadditive effects on stability and nonadditive effects on denatured-state structure as reflected in the changes observed in m_{GuHCl}. This is precisely what is found for each of the five classes of double mutants: $\Delta\Delta\Delta G$ correlates with $\Delta\Delta m$. For those doubles that are more stable than predicted on the assumption of additivity, m_{GuHCl} is also greater than predicted.

For the $m^+ \times m^+$ double-mutant class, the range in values of $\Delta\Delta\Delta G$ and $\Delta\Delta m$ is comparable to the measurement errors in these parameters, making it likely that the correlation in this case is a consequence of the isokinetic effect (Krug et al., 1976) that arises from the correlation of errors between two interdependent parameters obtained from the same data set. (The fact that the correlation coefficient is very close to 1.0 supports this conclusion.) For the three largest classes involving m^- mutants, this correlation is unlikely to be a result of the isokinetic effect because (1) the variations in $\Delta\Delta\Delta G$ and $\Delta\Delta m$ among the various double mutants are much larger than the errors in these parameters, (2) the observed slope of the plot of $\Delta\Delta\Delta G$ vs $\Delta\Delta m$ is considerably larger than that predicted for a correlation of the errors in these two parameters (which is approximately 2–3 kcal mol^{-1} m-$unit^{-1}$), and (3) only two negative values of $\Delta\Delta\Delta G$ are observed, whereas for an artifactual correlation there should be equal numbers of positive and negative values.

In an attempt to draw inferences about the molecular interactions underlying the patterns of nonadditivity reported here, we proceed to make the following assumptions: (1) Changes in m_{GuHCl} for single mutants reflect a sphere of perturbation affecting the structure of the denatured state. m^+ mutants disrupt part of the wild-type denatured-state structure, leading to an increase in solvent-exposed nonpolar surface, whereas m^- mutants change the denatured-state structure in a way that is equivalent to decreasing the exposed nonpolar surface. (2) Overlap between the two spheres of perturbation present in the denatured state of a double mutant is responsible for all of the nonadditivity observed for both Δm_{GuHCl} and $\Delta\Delta G_{H_2O}$. (Although some native-state interactions must occur for some mutants, especially those at positions 37, 79, 117, and 118, most mutant pairs are remote in space in the native state. So, in the interest of simplifying the interpretation of these data, we ignore all nonadditive effects on $\Delta\Delta G_{H_2O}$ which arise from interactions in the native state.) To these two assumptions we add the conclusion reached from previous studies of single mutants that (3), on average, a change in m_{GuHCl} of 1 unit (defined as the value of m_{GuHCl} for wild-type nuclease) *in either direction* lowers the free energy of the denatured state by 15.0 kcal/mol (Shortle et al., 1990; Green et al., 1992).

To graphically represent the interactions between a pair of mutations in two dimensions rather than three, a Venn diagram is used, with each mutation's sphere of perturbation represented by a circle. The part of the denatured-state structure that is not perturbed by either of the two mutations is represented by a light gray background. Regions of perturbed denatured structure that have changed to m^- structure are darkly shaded, regions that have changed to m^+ structure are highlighted in white, and regions that retain the wild-type m^0 structure are shaded light gray.

With this simple scheme, the component of $\Delta\Delta G_{H_2O}$ in the double mutant which derives from structural effects on the denatured state is equal to the silhouette formed by the overlapped pair of circles. Shading is not relevant to $\Delta\Delta G_{H_2O}$, since m^+ and m^- structures are equivalent in their effects on stability (assumption 3 above). The nonadditivity in $\Delta\Delta G_{H_2O}$, i.e., $\Delta\Delta\Delta G$, is proportional to the area of overlap. As shown in Figure 3, with this model, there are three ways of representing the overlap region which gives rise to the nonadditivity in Δm_{GuHCl} observed for $m^- \times m^-$ double mutations: (A) dark m^- shading, corresponding to a saturation of the m^- effect (if a region of perturbed structure is made m^- by one mutation, a second mutation causes no further change); (B) gray m^0 shading, corresponding to a cancellation of the m^- effects from the two mutations through conflicting structural perturbations; and (C) white m^+ highlighting, representing not just a cancellation of the m^- structural effects but also their transformation into m^+ structural effects.

An important quantitative feature of this model is that the three overlap modes differ with respect to the rates of change of $\Delta\Delta G_{H_2O}$ and Δm_{GuHCl} as the area of overlap between the two circles increases. For mode A, $\Delta\Delta G_{H_2O}$ and Δm_{GuHCl} decrease at equal rates; for mode B, $\Delta\Delta G_{H_2O}$ changes half as fast as Δm_{GuHCl}, because transformation of the overlap region to m^0 structure means twice as much m^- structure is lost and therefore does not contribute to Δm_{GuHCl}; and for mode C, $\Delta\Delta G_{H_2O}$ changes only at one-third the rate of Δm_{GuHCl} because effectively 3 times as much m^- structure is lost and unable contribute to Δm_{GuHCl}.

For the $m^- \times m^-$ double-mutant class, the average rate of change of $\Delta\Delta G_{H_2O}$ with respect of Δm_{GuHCl} (i.e., $\Delta\Delta\Delta G/$

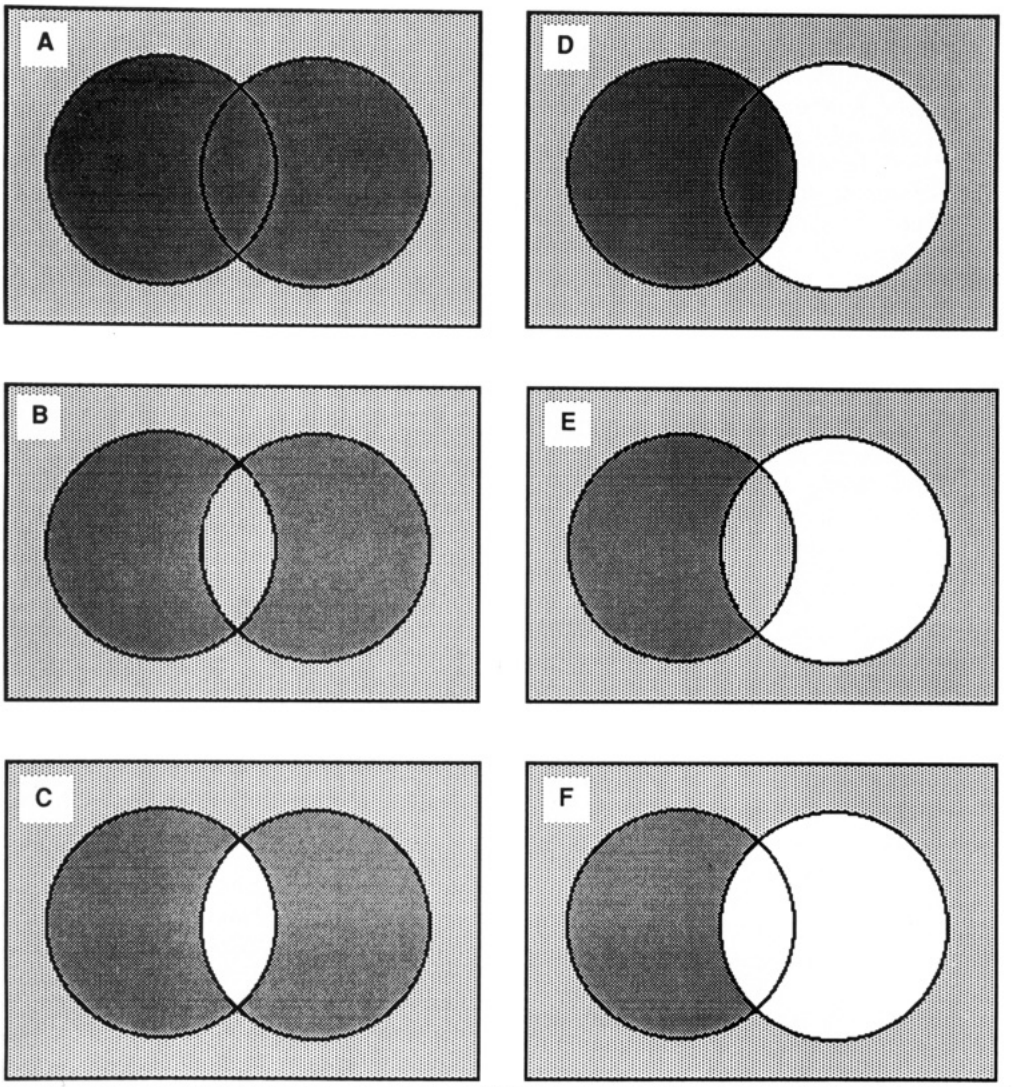

FIGURE 3: Venn diagram representation of the interactions between the spheres of structural perturbation in the denatured state of a double-mutant protein. The effect of each mutation is represented as a circle, with the unaffected component of structure indicated by the surrounding rectangle. The three hypothetical types of denatured-state structure are wild-type or m^0 structure (light gray), m^- structure (dark gray), and m^+ structure (white). Panels A–C correspond to the three possible states of the region of overlap for double mutants of the $m^- \times m^-$ class, and panels D–F correspond to the three possible states of the overlap region for members of the $m^- \times m^+$ class.

$\Delta\Delta m$) is 10.6 kcal mol^{-1} m-$unit^{-1}$, which is two-thirds of the expected value of 15.0 kcal mol^{-1} m-$unit^{-1}$ if mode A were the sole mechanism. Thus, some degree of saturation of the m^- effect in the overlap region must occur in some of these double mutants. Such saturation effects appear to be the only overlap mode that explains the remarkable nonadditivity of mutant combinations at positions 37, 79, and 118. An m^- mutation at position 37 can virtually mask the presence of one or two additional mutations at the remaining sites; all of the changes in Δm_{GuHCl} and the accompanying changes in $\Delta\Delta G_{H_2O}$ expected for the second and/or third mutations are nearly perfectly canceled. Any consistent model involving conflicting effects (overlap modes B and C) between each of three pairs of mutations has difficulty predicting the complete absence of additional effects of a third mutation. Yet for other doubles in this group, some cancellation or conflict of interactions in the overlap region presumably must occur to account for the smaller than predicted average value of $\Delta\Delta\Delta G/\Delta\Delta m$.

Similarly, three possible modes of overlap can explain the nonadditivity observed in the $m^- \times m^+$ double mutants (Figure 3D–F), again with the one variable being the structural state of this region. If one increases the overlap between the two circles, and the overlap region is darkly m^- shaded (mode D), Δm_{GuHCl} changes in the opposite direction from $\Delta\Delta G_{H_2O}$; m_{GuHCl} is lower than predicted on the assumption of additivity, and the stability is higher. For mode E, Δm_{GuHCl} remains constant (equal amounts of opposing m^+ and m^- components are lost on overlap), while the stability increases, and for mode F, Δm_{GuHCl} and $\Delta\Delta G_{H_2O}$ are both larger than predicted, leading to a double mutant that is more wild type than expected for both stability and m_{GuHCl}. For 9 of the 10 pairs in this class, the double mutant was found to be more stable and the m_{GuHCl} larger than predicted for additive behavior, suggesting that the m^+ effect dominates in the overlap region (Figure 3F). However, the average rate of change of $\Delta\Delta G_{H_2O}$ with respect to Δm_{GuHCl} is 4.1 kcal mol^{-1} m-$unit^{-1}$, which is only one-third the rate expected on the basis of the rate of 15.0 kcal mol^{-1} m-$unit^{-1}$ from single mutants. This suggests that this simple model based on circles of fixed size and shading is not sufficiently complex to represent all of the interactions in this case. Obviously, the model could be modified in a variety of ways to make Δm_{GuHCl} increase more rapidly than $\Delta\Delta G_{H_2O}$.

Additional evidence that the behavior of some pairs of mutants is more complex than allowed by this simple model comes from the $m^0 \times m^0$ double mutants. If each m^0 mutant were more or less equivalent to wild type, then the double

mutant should also be an m^0 mutant and the loss in stability should be additive (reflecting changes in native-state interactions which are not manifest in changes in m_{GuHCl}). However, five of the six $m^0 \times m^0$ double mutants exhibit an unequivocal m^+ effect, and all six show a higher value of m_{GuHCl} than predicted from the assumption of additivity. This pattern suggests that m^0 mutants are not without effect on the denatured state. Perhaps the simplest explanation is that regions of m^+ structure are present in some m^0 mutants but are masked by other regions of m^- structure of approximately the same area. In this case, the only evidence for such underlying hidden or cryptic effects on m_{GuHCl} in a single mutant with a wild-type value of m_{GuHCl} would be a loss in stability. However, in the presence of other mutations, such m^0 mutants could give rise to rather complex patterns of nonadditivity. Given the dominance of the m^+ effect over the m^- effect in overlap regions described above, the m^+ character of m^0 mutants might be manifest upon pairing with m^- mutants. Thus, the finding that $m^0 \times m^0$ mutants frequently have values of m_{GuHCl} that classify them as m^+ is consistent with this idea. In these cases, the m^- region of one m^0 mutant might overlap with m^+ region of the other m^0 mutant, leading to cancellation of some of the cryptic m^- character. Likewise, overlap of m^- regions would also lead to a larger than expected m_{GuHCl}, as is seen for the $m^- \times m^-$ mutants.

Additional evidence for cryptic m effects in m^0 mutants comes from the patterns of nonadditivity observed among the pairs of $m^- \times m^0$ mutants. For this large class of 30 mutant proteins, a spectrum of effects is seen. However, in all cases, the m_{GuHCl} of the double mutant is either essentially that predicted on the assumption of additivity or it is larger, as would be predicted if some m^0 mutants harbor cryptic m^+ or m^- regions which become manifest in the presence of the appropriate m^- region. Furthermore, for this class of double mutants, the rate of change in $\Delta\Delta G_{H_2O}$ with respect to Δm_{GuHCl} is 5.2 kcal mol^{-1} m-$unit^{-1}$, a value remarkably similar to that found for the $m^- \times m^+$ pairs. In other words, as a group, the m^0 mutants are behaving as if they are m^+ mutants under some, but not all, circumstances.

The extensive heterogeneity of this class of six mutants becomes apparent when effects in combination with five different m^- mutants are considered. For example, I72V has a value of m_{GuHCl} of 1.02 and a stability loss of 1.77 kcal/mol. In each of the five pairs, the $\Delta\Delta m$ is positive and varies from 0.09 to 0.14. Likewise, the very similar m^0 mutation I92V gives rise to values of $\Delta\Delta m$ that vary from 0.06 to 0.11. However, m^0 mutant Y85A only leads to a significant $\Delta\Delta m$ with two of the 5 m^- mutants; for I15V, a significant $\Delta\Delta m$ is seen with three m^- mutants, and for Y113A, a significant $\Delta\Delta$m is seen with four m^- mutants. For m^0 mutant A130G, effects on m_{GuHCl} and stability are close to being additive with all five m^- mutants.

Obviously, Venn diagrams fall short of a molecular description of the perturbations of denatured-state structure caused by m^+ and m^- mutations. Toward this end, a simple physical chemical model has been proposed (Green et al., 1992), one developed around the postulate that chain entropy and solvation of nonpolar surface are the two dominant energetic terms in the denatured state (Dill,1990). In this model, it was proposed that, during the evolution of a stable form of staphylococcal nuclease, the amino acid sequence of the wild-type protein has been optimized to confer on the denatured state a maximal free energy, presumably through structures that attempt to maximize exposure of nonpolar surface and minimize the entropy of the polypeptide chain.

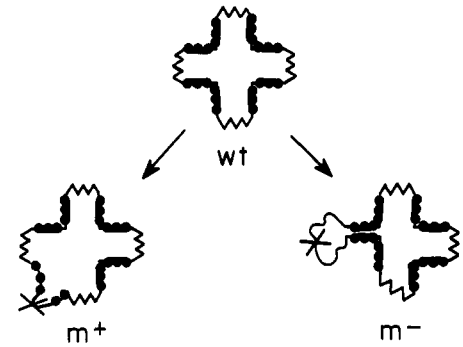

FIGURE 4: Schematic diagram of a model for the changes in denatured-state structure that accompany m^+ and m^- mutations (Green et al., 1992). The wild-type denatured state is postulated to possess an optimal balance between a low-chain entropy and a high exposure of hydrophobic surface. Thin lines represent relatively polar segments of chain that separate clusters of hydrophobic residues, which are represented by heavy lines and dark circles. m^+ mutations disrupt hydrophobic clusters, leading to an increase in both chain entropy and exposure of hydrophobic surface. Structured polar segments that act to separate hydrophobic clusters and thereby increase exposure of hydrophobic surface are disrupted by m^- mutations, leading to a decrease in exposure and an increase in chain entropy.

One simple way of representing the general features of this model is shown in Figure 4. The residual structure of the denatured state is proposed to consist of two parts: structured nonpolar regions indicated by dark lines and structured intervening regions with more polar character indicated by thin lines. To increase the free energy of the D state by maximizing exposure of nonpolar surface, the nonpolar regions are forced apart and into contact with water by the structures formed by the intervening regions. The effects of m^- mutations can then be interpreted as reducing the structure of an intervening region, thereby lowering the free energy of the denatured state through the combined effects of a loss in chain structure (a gain in chain entropy) and a reduction in nonpolar surface exposure (which lowers the value of m_{GuHCl}). Similarly, m^+ mutations can be interpreted as acting directly to reduce the structure of hydrophobic regions. In this case, the free energy of the denatured state would be lowered by the increase in chain entropy but increased by the greater exposure of nonpolar surface (which increases the value of m_{GuHCl}), the former presumably dominating over the latter.

Although this simple model is certainly not unique, it does successfully explain two features of the data. (1) m^- effects show saturation. If the structured intervening region that holds two hydrophobic clusters apart has been disrupted and the hydrophobic clusters have merged, little additional effect is expected from a second m^- mutation that perturbs this intervening region. (2) m^+ effects are dominant to m^- effects. If a hydrophobic cluster has been disrupted, the role of the structured intervening region is more or less eliminated, diminishing the potential effect of an m^- mutant on combination with an m^+ mutant.

The remarkable prevalence of nonadditive effects on both $\Delta\Delta G_{H_2O}$ and Δm_{GuHCl} among the 71 mutant pairs suggests that either there are only a small number of hydrophobic clusters and intervening regions or there is extensive cooperativity among the hydrophobic clusters so that a change in one cluster alters the consequences of changes at considerable distances away. It is hoped that a more complete picture of the complex interactions in the denatured state will be obtained from analysis of the wild-type nuclease and several of these mutants by NMR spectroscopy (unpublished data). If proteins are found to employ common structural motifs in the denatured

state to achieve an optimum balance between chain entropy and nonpolar surface exposure, the identification of such motifs might provide useful low-resolution "templates" for predicting the general features of a protein's native structure from its amino acid sequence.

ACKNOWLEDGMENT

We thank John Sondek for constructing and analyzing mutants I18M+T33S, I18M+A69T, and I18M+A90S, John Sondek, Gary Ackers, Wesley Stites, and Alan Meeker for helpful discussions, and Neil Clarke for his careful reading of the manuscript.

REFERENCES

Ackers, G. K., & Smith, F. R. (1985) *Annu. Rev. Biochem. 54*, 597–629.

Bowler, B. E., May, K., Zaragoza, T., York, P., Dong, A., & Caughey, W. S. (1993) *Biochemistry 32*, 183–190.

Dao-pin, S., Soderlind, E., Baase, W. A., Wozniak, J. A., Sauer, U., & Matthews, B.W. (1991) *J. Mol. Biol. 221*, 873–887.

Dill, K. A. (1990) *Biochemistry 29*, 7133–7155.

Dill, K. A., & Shortle, D. (1991) *Annu. Rev. Biochem. 60*, 795–825.

Eriksson, A. E., Baase, W. A., Zhang, X. J., Heinz, D. W., Blaber, M., Baldwin, E. P., & Matthews, B. W. (1992) *Science 255*, 178–183.

Fuchs, S., Cuatrecasas, P., & Anfinsen, C. B. (1967) *J. Biol. Chem. 242*, 4768–4770.

Goldenberg, D. P. (1988) *Annu. Rev. Biophys. Biophys. Chem. 17*, 481–507.

Green, S. M., Meeker, A. K., & Shortle, D. (1992) *Biochemistry 31*, 5717–5728.

Horovitz, A., Serrano, L., Avron, B., Bycroft, M., & Fersht, A. R. (1990) *J. Mol. Biol. 216*, 1031–1044.

Hynes, T. R., & Fox, R. O. (1991) *Proteins: Struct., Funct., Genet. 10*, 92–105.

Krug, R. R., Hunter, W. G., & Grieger, R. A. (1976) *J. Phys. Chem. 80*, 2335–2341.

Kunkel, T. A. (1985) *Proc. Natl. Acad. Sci. U.S.A. 82*, 488–492.

Loll, P. J., & Lattman, E. E. (1989) *Proteins: Struct., Funct., Genet. 5*, 183–201.

Matthews, B. W. (1987) *Biochemistry 26*, 6885–6888.

Mildvan, A. S., Weber, D. J., & Kuliopulos, A. (1992) *Arch. Biochem. Biophys. 294*, 327–340.

Perry, K. M., Onuffer, J. J., Gittelman, M. S., Barmat, L., & Matthews, C. R. (1989) *Biochemistry 28*, 7961–7968.

Richardson, J. S. (1981) *Adv. Protein Chem. 34*, 167–339.

Sandberg, W. S., & Terwilliger, T. C. (1989) *Science 245*, 54–57.

Serrano, L., Horovitz, A., Avron, B., Bycroft, M., & Fersht, A. R. (1990) *Biochemistry 29*, 9343–9352.

Serrano, L., Bycroft, M., & Fersht, A. R. (1991) *J. Mol. Biol. 218*, 465–475.

Shirley, B. A., Stanssen, P., Steyaert, J., & Pace, C. N. (1989) *J. Biol. Chem. 264*, 11621–11625.

Shortle, D. (1989) *J. Biol. Chem. 264*, 5315–5318.

Shortle, D. (1992) *Q. Rev. Biophys. 25*, 205–250.

Shortle, D. (1993) *Curr. Opin. Struct. Biol. 3*, 66–74.

Shortle, D., & Meeker, A. K. (1986) *Proteins: Struct., Funct., Genet. 1*, 81–89.

Shortle, D., & Meeker, A. K. (1989) *Biochemistry 28*, 936–944.

Shortle, D., Meeker, A. K., & Gerring, S. L. (1989) *Arch. Biochem. Biophys. 272*, 103–113.

Shortle, D., Stites, W. E., & Meeker, A. (1990) *Biochemistry 29*, 8033–8041.

Stearman, R. S., Frankel, A. D., Freire, E., Liu, B., & Pabo, C. O. (1988) *Biochemistry 27*, 7571–7574.

Wells, J. A. (1990) *Biochemistry 29*, 8509–8517.

Zhang, X. J., Baase, W. A., & Matthews, B. W. (1991) *Biochemistry 30*, 2012–2017.

Zhang, X. J., Baase, W. A., & Matthews, B. W. (1992) *Protein Sci. 1*, 761–776.